Available online at www.sciencedirect.com
SCIENCE DIRECT
solid state communications
Solid State Communications 136 (2005) 572–575
www.elsevier.com/locate/ssc

External ac-signal-controlled dynamics of electric field domains in a GaAs/AlAs superlattice

H.T. He[a], Z.Z. Sun[a], X.R. Wang[a], Y.Q. Wang[b], W.K. Ge[a], J.N. Wang[a,*]

[a] Physics Department, the Hong Kong University of Science and Technology, Clear Water Bay, Hong Kong, China
[b] Institute of Solid State Physics, Chinese Academy of Sciences, Hefei, Anhui, China

Received 2 September 2005; accepted 28 September 2005 by A.H. MacDonald

Available online 19 October 2005

Abstract

The dynamics of the electric field domain of an ac-driven weakly coupled GaAs/AlAs superlattice is investigated. The ac-induced generation and annihilation of self-sustained current oscillations (SSCOs) is observed. The calculation using the discrete drift model based on a phenomenological drift velocity curve agrees well with the experimental observations. The localization of the domain wall at high ac frequencies is responsible for the disappearance of SSCOs. It indicates that the external ac signal is an additional important control parameter in the dynamics of weakly coupled superlattices besides the carrier concentration, sample temperature, and applied transverse magnetic field.

PACS: 73.40.Gk; 73.61.−r

Keywords: D. Tunneling; D. Electronic transport; A. Quantum wells

Since the pioneering work of Esaki and Chang [1,2], the vertical transport of weakly coupled superlattices (SLs) has been shown to exhibit many interesting behaviors. It includes the sawtooth-like current–voltage (*I–V*) characteristics [2,3], self-sustained current oscillation (SSCO) [4–7] and chaos [8]. It is understood that the formation of stable electric field domains (EFDs) in SL is responsible for the occurrence of sawtooth-like *I–V* characteristics and the SSCO is attributed to the traveling of the domain boundary within SL [9,10], which can be induced by varying the doping density (N_D) [5], the temperature (T) or the transverse magnetic field (B) [6,7]. A detailed review can be found in Ref. [11]. Since the SSCO has potential applications in microwave devices, the understanding of the interaction of an external ac signal with the SSCO is essential. In previous work, the frequency locking phenomena have been demonstrated in the study of this interaction [12,13].

It has been found that in the transition from static to dynamic EFDs, the so-called dynamic voltage band (DVB) begins to emerge at the lower voltage side within each sawtooth-like current branch, squeezing out the static voltage band (SVB) [6]. As long as the dc bias lies within these DVBs, SSCOs are observed. However, the external ac influence on these DVBs has never been studied. This is the motivation of this work. With an additional ac bias applied, the emerging and expansion of DVB with increasing ac amplitude (V_{ac}) and the quenching of DVB at high ac frequencies (ω_{ac}) are observed. Using the widely adopted discrete drift (DD) model [9,10], the ac-induced expansion of DVBs is simulated numerically based on a phenomenological drift velocity curve. The localization of domain walls at high ω_{ac} is considered to be responsible for the quenching of DVBs.

* Corresponding author.
E-mail address: phjwang@ust.hk (J.N. Wang).

0038-1098/$ - see front matter
doi:10.1016/j.ssc.2005.09.036

The GaAs/AlAs SL sample used in this work was grown by molecular beam epitaxy. It consists of 30 periods of 14 nm GaAs well and 4 nm AlAs barrier and is sandwiched between two n^+-GaAs layers. The central 10 nm of each GaAs well was doped with Si ($n=2\times10^{17}\ \mathrm{cm}^{-3}$). The sample was fabricated into $0.2\times0.2\ \mathrm{mm}^2$ mesas. The sample temperature is fixed at 97 K, at which the temperature-induced DVB is observed in the time-averaged *I–V* curve as shown in Fig. 1. For clarity, only a part of *I–V* curve from the first sequential tunneling plateau is given. The free *I–V* curve shows two complete sawtooth-like branches (labeled ‘A’ and ‘B’ in the figure) and the presence of one DVB in the ‘C’ branch as indicated. The SSCO from this DVB is shown in the inset of Fig. 1 with dc bias fixed at 537 mV. The measured SSCO frequency ω_0 is 18 KHz.

The influence of the small external ac bias on the DVB is investigated under fixed ω_{ac} (18 KHz) and different ac amplitudes V_{ac}. As shown in Fig. 1, the ac-induced DVBs are evident in branch A and B and with increasing V_{ac} the expansion of DVBs in the expense of SVBs within each branch (A, B and C) are clearly observed. These DVBs finally join up together at $V_{ac}=13$ mV. Thus, the whole voltage region become dynamic and SSCOs can be observed through out the plateau.

The DD mode [9,10] has been shown to account for the vertical charge transport in weakly coupled SLs quite well, such as the sawtooth-like *I–V* characteristics and SSCOs. According to this model, the dynamics of weakly coupled SLs is governed by the following equations:

$$\varepsilon\frac{\mathrm{d}F_i}{\mathrm{d}t}+\frac{en_iv(F_i)}{l}=J(t),\quad i=1,\ldots,N \tag{1}$$

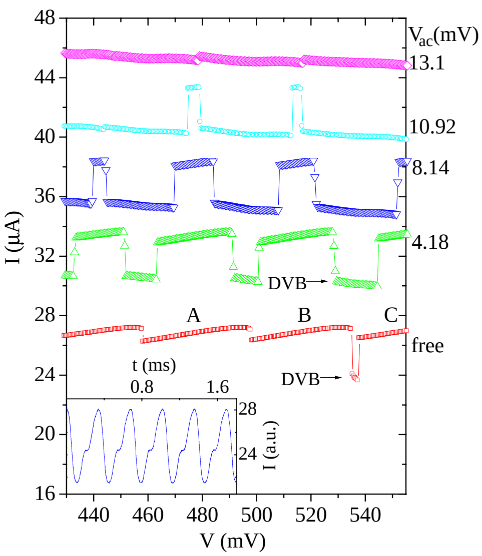

Fig. 1. Time-averaged *I–V* curves under different ac conditions. The corresponding V_{ac} in the unit of mV is indicated. Curves are offset for clarity and lines are guides for the eye. Inset: the SSCO observed in the DVB of branch C when no ac bias is applied.

$$F_i-F_{i-1}=\frac{e}{\varepsilon}(n_i-N_\mathrm{D}),\quad i=i,\ldots,N \tag{2}$$

$$l\sum_{i=0}^{N}F_i=V_t=V+V_{ac}\sin(\omega_{ac}t) \tag{3}$$

$$n_1=N_\mathrm{D}+\delta\approx N_\mathrm{D}+10^{-3}N_\mathrm{D} \tag{4}$$

where ε, e, N_D and l are the well permittivity, the electron charge, the two-dimensional (2D) doping density in the wells, and the SL period, respectively. In the simulation, these parameters are chosen according to the specifications of the sample. Eq. (1) shows the total current density $J(t)$ consists of a displacement current and a drift current. Eq. (2) is the Poisson equation. n_i is the 2D electron density in the ith well and F_i is the average electric field across the ith period. The bias constraint condition is given by Eq. (3), where V_t is the total bias applied to the contacts. To include the ac influence in this model, V_t consists of a dc bias V and an ac component $V_{ac}\sin(\omega_{ac}t)$. V_{ac} and ω_{ac} are the amplitude and frequency of the ac signal, respectively. Eq. (4) is the assumed phenomenological boundary condition, where δ accounts for the excess electron density in the first well due to the tunneling from the highly doped contact region. Finally, a phenomenological drift velocity curve $v(F)$ shown in the inset of Fig. 2 is adopted in the calculation.

The numerical result is shown in Fig. 2. For clarity, only two current branches are shown. When no ac signal is applied ($V_{ac}=0$), the calculated current density J as the function of the dc bias V already exhibits the alternation of DVBs and SVBs, as shown by the open square curve in Fig. 2. The frequency of SSCOs in DVBs is around 120 KHz. However, with an extra ac signal applied ($\omega_{ac}=$ 120 KHz), each DVB expands with the increasing ac amplitude V_{ac}. As V_{ac} is increased to 0.0014 V, the DVBs start to join up together. These results are in good agreement with the experimental observations. This implies that the ac-induced expansion of DVB is the intrinsic effect of ac-driven weakly coupled SLs and it is not due to the coupling of SLs with the external electric circuit. Therefore, it clearly

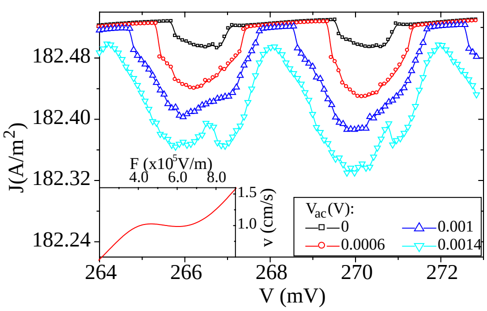

Fig. 2. The calculated DVB expansion at the ac amplitudes indicated. Lines are guides for the eye. The inset is the phenomenological drift velocity curve adopted in the numerical calculation.